International Atomic Energy Agency

INDC(CCP)-21/L

FEI - 274

INDC INTERNATIONAL NUCLEAR DATA COMMITTEE

ABSOLUTE MEASUREMENTS OF α FOR URANIUM-235 AND PLUTONIUM-239 IN THE 10 keV-1 MeV NEUTRON ENERGY RANGE

V.N. Kononov, E.D. Poletaev, Yu.S. Prokopets,
A.A. Metlev and Yu.Ya. Stavissky
Institute of Physics and Energetics
Obninsk, 1971

Translated by IAEA
from a Russian original
February 1972

INDC(CCP)-21/L

FEI - 274

ABSOLUTE MEASUREMENTS OF α FOR URANIUM-235 AND PLUTONIUM-239 IN THE 10 keV-1 MeV NEUTRON ENERGY RANGE

V.N. Kononov, E.D. Poletaev, Yu.S. Prokopets,
A.A. Metlev and Yu.Ya. Stavissky
Institute of Physics and Energetics
Obninsk, 1971

Translated by IAEA
from a Russian original
February 1972

ABSTRACT

The article describes the method and results of experiments designed for measuring α, the ratio of the radiative capture and fission cross-sections ($\alpha = \sigma_c/\sigma_f$), for uranium-235 and plutonium-239 in the 10 keV-1 MeV neutron energy range. The measurements were carried out on the Institute's EG-1 Van de Graaff pulsed accelerator. A pulsed neutron beam was used to identify radiative capture and fission events and to measure neutron energy from the time of flight. Capture and fission events were detected from the prompt gamma-rays with the help of a scintillation tank. The capture and fission events were identified by the same detector, by recording fission neutrons after slowing down and absorption in cadmium. The measurement method is absolute. The experimental accuracy of the α values obtained is 10-15%.

I. INTRODUCTION

The ratio of the cross-section for radiative capture of neutrons to the fission cross-section ($\alpha = \sigma_c/\sigma_f$) is one of the most important nuclear-physics constants used in fast reactor calculations. The value of α determines, to a considerable extent, the breeding ratio of the nuclear fuel and consequently the economic characteristics of fast breeder reactors. Since the neutron spectrum in such reactors ranges from a few keV to several hundred keV, we need to know the value of α over a wide range of neutron energies for the reactor calculations. Furthermore, present reactor calculation methods require highly accurate determinations of α. For example, Greebler [1] considers that the accuracy of α determinations for ^{239}Pu should be about 3% in the 1-100 keV range and about 5% in the 100-1000 keV range.

At present, there are several experimental methods of deriving α values for the main isotopes used as nuclear fuel. A feature common to all the familiar methods is that we measure experimentally not the value of α alone but the value of $(\alpha + K)$. The accuracy of α thus depends very greatly on the absolute value of the constant in the experimental method, K.

Direct experiments on accumulation and experiments aimed at measuring radioactivity, usually called integral methods, give a value of α which is averaged over the neutron spectrum of the specific type of reactor used for the experiment.

In the case of monoenergetic neutrons, the value of α can be obtained from measurements of $\eta = \frac{\bar{\nu}}{1+\alpha}$, and in experiments giving direct measurements of α.

In the fast neutron range, η has usually been measured on photoneutron sources by the spherical-geometry method [2-4], the experimental accuracy of α obtained from such experiments being about 10%. An advantage of the spherical-geometry method is that an absolute value of α can be obtained. However, its use has so far been limited by the availability of photoneutron sources.

Where direct measurements of α are concerned, the problem is to obtain simultaneous measurements of the neutron radiative capture cross-section (from the capture gamma rays) and of the fission cross-section. This method is quite universal but gives rise to difficulties because the capture gamma ray detector also records fission events with great efficiency. Therefore,

in most experiments of this type one actually measures the neutron absorption cross-section and the fission cross-section, the quantity measured being, in the best case, $\alpha+1$. Moreover, in most experiments it has not been possible to measure the efficiency of detection of fission and capture events, so that in fact only relative measurements of α are made. An exception is the method which uses a cadmium-filled scintillation tank to detect capture and fission events. This is an absolute method - a particularly important advantage in measuring α for fast neutrons - and a value close to α ($\alpha + 0.15 \div 0.3$) is measured in the experiment. It is this method which is used in the present work.

II. METHOD OF MEASURING THE VALUE OF α

The method of measuring the value of α is based on the use of a large cadmium- or gadolinium-filled scintillation detector (scintillation tank) [5-6], which makes it possible to record, with high efficiency, the prompt gamma rays produced by radiative capture of neutrons and fission events, as well as fission neutrons.

The fission and neutron capture events in a sample of fissionable isotope placed at the centre of the scintillation tank are recorded from the prompt capture and fission gamma rays. Neutron capture is characterized exclusively by prompt pulses occurring during the recording of a cascade of capture gamma rays. Fission events, apart from the prompt pulses generated by fission gamma rays, may be accompanied by the appearance during some time interval after fission ("expectation time") of one or more pulses associated with the recording of fission neutrons after these have been slowed down and absorbed by cadmium nuclei. This characteristic is used for identifying the fission and capture events and thus permits a direct measurement of α.

In actual conditions, not all fission events are marked by the detection of fission neutrons in the expectation time interval, and some fission events will accordingly be identified as capture events. Moreover, some capture events may be accompanied by the appearance of a random background pulse in the expectation time interval and identified as fission events. Considering these facts, the number of single events recorded by the detector (N_1) and the number of events accompanied by the appearance of at least one pulse (N_2) in the expectation time interval can be written as

$$N_1 = \varepsilon_{\gamma c} n_c - \varepsilon_{\gamma c} P + \varepsilon_{\gamma f} n_f C (1-P) \qquad (1)$$

$$N_2 = \varepsilon_{\gamma f} n_f - \varepsilon_{\gamma f} n_f C (1-P) + \varepsilon_{\gamma c} n_c P \qquad (2)$$

where n_c and n_f are the number of neutron capture and fission events in the sample; $\varepsilon_{\gamma c}$ and $\varepsilon_{\gamma f}$ are the efficiency of recording capture and fission events from prompt gamma rays; C is the probability that a fission event will not be accompanied by the detection of fission neutrons in the expectation time interval; and P is the probability that an event will be accompanied by a random background pulse in the expectation time interval.

The value of α can be determined from relations (1) and (2):

$$\alpha = \frac{n_c}{n_f} = \frac{\varepsilon_{\gamma f}}{\varepsilon_{\gamma c}} \cdot \frac{N_1/N_2[1-C(1-P)] - C(1-P)}{(1-P) - N_1 P/N_2} \qquad (3)$$

In order to obtain the absolute value of α, we thus need not only to measure the number of events, N_1 and N_2, but also to determine the probabilities C and P and the ratio of the detection efficiencies for fission and capture events, $\varepsilon_{\gamma f}/\varepsilon_{\gamma c}$.

The ratio of efficiencies $\varepsilon_{\gamma f}/\varepsilon_{\gamma c}$ for the scintillation tank is close to 1 and can be determined from measurements of the amplitude spectra of capture and fission events.

The probability (C) of a fission event not being accompanied by detection of fission neutrons during the expectation time can be measured if the sample is replaced by a fission chamber and only those events (N_1 and N_2) are recorded which coincide with the pulse from the fission chamber. In this case

$$N_1^k = \varepsilon_{\gamma f} n_f^k C(1-P) \qquad (4)$$

$$N_2^k = \varepsilon_{\gamma f} n_f^k - \varepsilon_{\gamma f} n_f^k C(1-P) \qquad (5)$$

where n_f^k is the number of fission events recorded by the fission chamber.

Hence

$$C = \frac{N_1^k}{(N_1^k + N_2^k)(1-P)} \qquad (6)$$

The probability (P) of a recorded event being accompanied by a background pulse in the expectation interval can also be determined experimentally. For this purpose the associate pulse expectation circuit must be triggered by random pulses which are not due to fission and capture events.

A brief consideration of the α measurement method using a cadmium-filled scintillation tank shows its important advantages:

1. The method is absolute;
2. The quantity measured in the experiment is ~ (α + C), where C is small because of the high efficiency of recording fission events from fission neutrons. This fact is particularly important in measurements involving fast neutrons, for which α is small;
3. The method is highly sensitive owing to the high efficiency of recording capture and fission events from prompt gamma rays;
4. Since the scintillation tank is actually a full gamma absorption detector, the method is not very sensitive to possible changes in the spectrum of capture gamma rays for different neutron energies.

Along with these advantages, however, the cadmium-filled scintillation tank has a major disadvantage - a high background due to neutrons scattered in the sample. However, the use of a pulsed beam of neutrons obtained from the $^{7}Li(p,n)^{7}Be$ and $T(p,n)^{3}He$ reactions in electrostatic accelerators has made it possible to obtain satisfactory signal-to-background ratios, especially in the case of monoenergetic neutrons. Moreover, by using the time-of-flight method on Van de Graaff pulsed accelerators to measure neutron energy, we can measure α in the 10-100 keV energy range where there are no convenient sources of monoenergetic neutrons and other types of neutron spectrometer based on the time-of-flight principle are still not very efficient.

III. DESCRIPTION OF THE EXPERIMENT

A. Neutron source

The measurements of α for ^{235}U and ^{239}Pu were performed on the EG-1 Van de Graaff pulsed accelerator belonging to the Institute of Physics and Energetics. The pulsed accelerator regime was obtained by chopping the ion beam from a high-current ion source at the accelerator tube input [7]. The parameters of the proton beam on the accelerator target during the main measurements were as follows: current pulse duration 20 nsec, current flow in the pulse ~ 1 mA and pulse repetition rate ~ 300 kHz.

The $^{7}Li(p,n)^{7}Be$ and $T(p,n)^{3}He$ reactions were used as neutron sources. In the 10-70 keV neutron energy range, the experiment was performed on a continuous spectrum of neutrons obtained from a "thick" lithium target. The

neutron energy was measured here by the time-of-flight method. In the 110 keV-1 MeV neutron energy range the experiment was performed on monoenergetic neutrons and the time-of-flight method was used only to eliminate the gamma ray background of the accelerator target and to distinguish the capture and fission effect against the background of neutrons scattered in the sample. Standard T-Ti targets and targets of metallic lithium were used, the lithium being applied on a tantalum substrate by vacuum dispersion from an evaporator placed inside the ion tube in the immediate vicinity of the target. The use of metallic lithium targets increased the neutron yield by a factor of about three in comparison with LiF targets and considerably reduced the gamma ray load on the detector from (p,γ) reactions.

A diagram of the experimental unit is shown in Fig. 1. The neutron beam obtained from the accelerator target is shaped by means of a collimator and passes through the central channel of the detector, in which the fissionable isotope sample is located. The path length from target to sample is 1.125 m. The resolution of the neutron energy measurement was thus 18 nsec/m.

B. Detector

The detector is a scintillation tank with a capacity of 400 litres, the central part of which contains a cylindrical chamber 200 mm in diameter filled with an aqueous solution of cadmium nitrate (cadmium nucleus concentration H:Cd = 100:1). This part of the detector acts as a converter in neutron recording. The lifetime distribution of fission neutrons in the detector, measured with a ^{252}Cf fission chamber, is shown in Fig. 2. On the basis of this distribution, the duration of the expectation interval for associated pulses is selected as 6 μsec. About 80% of the pulses due to fission neutron detection, occur in this interval.

As a scintillator, we used a solution of 4 g/litre p-terphenyl and 0.5 g/litre POPOP in toluene. To exclude the recording of fission neutrons with long lifetimes, which occurs as a result of diffusion of some of the fission neutrons entering the scintillator into the cadmium-filled region, we added to the scintillator 1.5 litres of ^{10}B-enriched trimethyl borate. This enabled us to eliminate the "tail" in the lifetime distribution (Fig. 2) attributable to neutrons which play no role in the identification of fission events and give rise to an additional background.

The inner surfaces of the detector are coated with a reflector of glazed enamel applied to a titanium dioxide base. The sensitive volume of the detector is scanned by eight FEU-49 photomultipliers with photocathodes 170 mm in diameter. The photomultipliers are positioned in direct optical contact with the scintillator. The output signals of all the photomultipliers are summed linearly into one common channel. The time resolution of the detector measured on the basis of coincidence with a fast-acting ^{252}Cf fission ionization chamber [8] was found to be 11 nsec for a dynamic pulse amplitude range of five.

In order to reduce the background due to cosmic rays and to gamma rays from the collimator and the target, the detector is surrounded by a lead shield 15 cm in thickness.

The most important property of the scintillation tank is its high efficiency in recording capture and fission events from prompt gamma rays. Fig. 3 shows the probability ε_{o1} - calculated for the detector used in the experiment - at least one interaction taking place in the scintillator for a single gamma quantum with energy E_γ. Obviously, ε_{o1} is the detection efficiency for recording a single gamma quantum given a zero threshold in the recording apparatus. Since several gamma quanta are emitted simultaneously during radiative capture or fission, the efficiency ε_{o1} of recording such events at zero threshold and the multiplicity of gamma quanta M are connected by the following relation:

$$\varepsilon_o = 1 - (1 - \varepsilon_{o1})^M \qquad (7)$$

Fig. 4 shows the function $\varepsilon_o(M)$ obtained for the detector on the assumption that the energy distribution in the cascade is uniform and the total cascade energy is 6.4 MeV.

At present, no experimental data are available on the spectra and average number of gamma quanta emitted during neutron capture in ^{235}U and ^{239}Pu. Therefore, we performed evaluations of average multiplicity, using level density data obtained in statistical theory and assuming that all gamma ray transitions are dipole transitions. These evaluations yielded an average multiplicity of $M = 4.8$ for capture gamma quanta in ^{235}U and ^{239}Pu. Assuming that the dispersion of the distribution P(M) is of the order of 1, the efficiency of recording capture events at zero threshold in the detector used is $\varepsilon_{oc} = 0.94$. If we assume an average multiplicity of $M = 4$, the efficiency will be $\varepsilon_{oc} = 0.9$.

Thus, the efficiency with which our detector records neutron capture events in ^{235}U and ^{239}Pu at zero threshold does not depend greatly on the average number of gamma quanta per capture event, and the evaluation of ε_{oc} at 0.92 ± 0.04 is realistic.

The average multiplicity and total energy of fission gamma rays have been measured by several authors [9]. Using these data, we determined the efficiency of recording fission events from prompt fission gamma rays at zero threshold as $\varepsilon_{of} = 0.98 \pm 0.01$.

In actual experimental conditions, photomultiplier noise and the high background in the low-energy range due to the radioactivity of the sample and cosmic rays make it necessary to set a fairly high threshold for recording detector pulses. Considering this point, we can write the ratio between the efficiencies of recording fission and capture events with the scintillation tank as

$$\frac{\varepsilon_{\gamma f}}{\varepsilon_{\gamma c}} = \frac{\varepsilon_{of}}{\varepsilon_{oc}} \cdot \frac{f_f}{f_c} \qquad (8)$$

where f_f and f_c are the fractions of pulses in the amplitude spectrum lying above the recording threshold at which the number of fission and capture events was measured.

Thus, to get an absolute determination of the ratio of recording efficiencies, $\varepsilon_{\gamma f}/\varepsilon_{\gamma c}$, we must not only carry out the above evaluations of ε_{of} and ε_{oc} but also measure the amplitude spectra of the detector pulses corresponding to the recording of fission and capture events to the lowest possible amplitude values, so that the spectra can be extrapolated to the zero threshold.

C. Electronic apparatus

The electronic apparatus used in the experiment must allow:

1. Measurement of neutron energy by the time-of-flight method;
2. Identification of the time spectra of events N_1 and N_2 from the associated pulses in the expectation time interval;
3. Measurement of the probability of a fission event not being accompanied by the recording of fission neutrons in the expectation interval (C);
4. Measurement of the probability of recording a random background pulse (P) in the expectation interval;

5. Measurement of the amplitude spectra of pulses corresponding to the recording of fission and capture events.

A block diagram of the electronic apparatus used in this experiment is shown in Figs 5 and 6.

The detector pulses go to the fast linear gate (FLG), the threshold of which is set at about 0.5 MeV in measurements with ^{235}U and about 0.9 MeV in measurements with ^{239}Pu. The fast linear gate makes it possible to exclude multiple superpositions of low-amplitude pulses, a particularly important point in measurements with ^{239}Pu samples, which emit about 4×10^7 gamma quanta per second in the 100-500 keV energy range.

The current pulses from the detector, after passing through the FLG, are integrated and enter the linear channel of the system. From another output of the FLG "time" signals which determine the instant of recording events in the detector go to the time channel of the system.

Let us consider the order of logical operations occurring in the device during the measurement of time spectra (Fig. 5).

Current pulses from the accelerator target marking the instant at which a neutron burst is generated are amplified by broad-band current amplifiers [8] and shaped (S). After the delay line DL, pedestal pulses open the fast gating circuit ("fast gate"), and admit detector pulses into the time-analysis circuit for just 1 μsec after the neutron burst. This time interval corresponds to the time of flight to the sample of all neutrons with energy higher than 8 keV.

The fast gating circuit can thus reduce the magnitude of the recorded background by a factor of 3.5. Furthermore, the fast gate is used for blocking the time-analysis circuit during the information processing time (expectation time of associated pulses and analyser dead time).

After passing through the fast gate, the detector signal starts the time-amplitude converter (TAC), which operates on the "start-stop" principle. Additionally-delayed pedestal pulses (DL_2) from the accelerator target are used as stop signals. The output pulses from the TAC go to the input of the multichannel amplitude analyser.

In the linear channel of the system, the detector pulses are amplified (A) and go to the differential discriminator (DD), which sets a range of detector pulse amplitudes within which time analysis is permitted.

To obtain a maximum effect-to-background ratio, the DD thresholds were set at 2.5-13 MeV.

Moreover, having passed through the fast gate, the detector pulses after 0.3 μsec (DL_3) start the associated pulse expectation circuit, which remains open for 6 μsec. If during this time a single detector pulse arrives at the input of the expectation circuit, the event under time analysis is identified as an N_2 event and an instruction to switch the analyser memory group ("Selection of plane I") is generated in the expectation circuit. Thus, N_1 and N_2 events are analysed by the same input units but recorded in different analyser memory groups.

The probability of a random background pulse (P) appearing in the expectation time interval is measured during the experiment by means of a random-pulse generator (RPG).

Passing through the fast gate, the RPG pulses perform random starting of the associated pulse expectation circuit. The random starts of the expectation circuit are selected by the coincidence circuit CC_1, while the detector pulses arriving in these expectation intervals are selected by circuit CC_2.

Thus, P is determined as the ratio of the readings on scalers SC_1 and SC_2. Because of the anticoincidence circuit AC in the control channel, the random pulses are not recorded in the analyser.

Such a circuit enables us to measure probability P throughout the experiment. This is an important advantage, since the background load on the detector may change owing to variability of the current on the target during the experiment.

The probability of a fission event not being accompanied by neutron recording (C) is measured in the experiment when the sample is replaced by the fission chamber. Coincidence circuit CC_3 in the control channel is used to select from all events recorded by the detector only those associated with fission.

Fig. 7 shows the time spectra of N_1 and N_2 events obtained in measurements with a ^{239}Pu sample.

To obtain the amplitude spectra of capture and fission events we must measure the amplitude spectra of the detector pulses in two time intervals, "effect + background" and "background", for both N_1 and N_2 events.

The block diagram of the experiment designed to measure amplitude spectra is shown in Fig. 6.

As in the measurement of time spectra, the detector pulses, after passing through the FLG, are directed into two channels. In the linear channel, the current pulses are integrated and amplified and go to the input of the multichannel amplitude analyser.

In the time channel, the pulses that have passed through the fast gate enter the TAC and start the associated pulse expectation circuit with which N_1 and N_2 events are identified. The TAC output pulses go to the two differential discriminators DD_1 and DD_2 and are used to distinguish the equal time intervals, "effect + background" and "background", in which amplitude analysis is permitted. The signal which operates DD_1 is also used as an instruction for switching the analyser memory group ("Selection of plane II"). Depending on the combination of the two instructions, "Selection of plane I" and "Selection of plane II", the information under analysis is recorded in one of the four groups (planes) of the analyser storage. All four amplitude spectra ("effect + background" N_1, "background" N_1, "effect + background" N_2, "background" N_2) are thus measured simultaneously with the help of the same input devices.

Probability P is determined with the help of the random-pulse generator, as in the measurement of time spectra.

Moreover, the RPG is also used here for measuring window widths in the discriminators DD_1 and DD_2. Since the random pulses at the TAC output form a "white" spectrum, the number of random pulses passing through the discriminators and measured by scalers SC_3 and SC_4 during the experiment is proportional to their window widths. Consequently, errors due to instability of the discrimination thresholds in the discriminators can be avoided.

The analyser is blocked the instant the RPG signal acts in the system. The anticoincidence circuit AC in the control channel is used for this purpose.

D. Samples

We used a metallic ^{239}Pu sample consisting of four disks 40 mm in diameter with a total weight of 14.5 g. Thus, the sample thickness was 2.9×10^{-3} nuclei/barn.

The sample was packed in a stainless steel container made of 25 μ foil. The sample and backing scattered about 3.5% of the incident neutrons. The ^{240}Pu content of the sample was 0.2%.

The ^{235}U sample was made of U_3O_8 90.3% enriched in ^{235}U. Before preparation of the sample the U_3O_8 was purified three times by ether extraction to remove decay products. This operation considerably reduced the gamma ray background due to the sample's natural radioactivity.

The sample was packed in an aluminium container 40 mm in diameter with a wall thickness of about 0.5 mm. The weight of U_3O_8 in the sample was 24.4 g. The sample thickness in terms of ^{235}U nuclei was 4.1×10^{-3} nuclei/barn. The sample and backing scattered about 10% of the incident neutrons.

Apart from the working samples, we made equivalent lead and carbon scatterers which were backed in exactly the same way as the fissionable isotope samples.

IV. MEASUREMENT RESULTS

A. Measurement of C

In measuring the probability of fission not being accompanied by the recording of fission neutrons (C), we used fast fission chambers [8] with ^{235}U and ^{239}Pu layers. The uranium chamber contained 100 mg of ^{235}U and had a fission event recording efficiency of about 95%. In the plutonium chamber we placed 50 mg of ^{239}Pu containing 2% ^{240}Pu and the recording efficiency was about 70%.

Moreover, throughout the experiment we carried out periodic measurements of probability C for ^{252}Cf which were used for verifying the stability of the experimental conditions. In this case, the pulses from spontaneous fissions recorded by the ionization chamber containing ^{252}Cf were used as pedestal pulses and applied to "Input I" of the measurement apparatus (Figs 5 and 6).

The measurements of probability C were performed on a continuous neutron spectrum, and the resulting experimental value of C represents an average for the 30-70 keV neutron energy range.

The measurement conditions applied to the chamber and sample of a given isotope were kept rigorously the same. However, the experiments with ^{235}U and ^{239}Pu were performed at different FLG thresholds, so that the values of C for ^{235}U and ^{239}Pu cannot be compared.

The measurements of C are given in Fig. 8 and Table 1.

Table 1.
Values of C and ε obtained in experiments with different isotopes

Isotope	$\bar{\nu}$	C_{exp}	ε	$\bar{\varepsilon}$	Remarks
^{239}Pu	2.874	0.2955 ± 0.0073	0.3798	0.3864	For experiments with
^{240}Pu	2.150	0.3985 ± 0.0002	0.3910	± 0.0034	^{239}Pu sample
^{252}Cf	3.760	0.1932 ± 0.00012	0.3885		
^{235}U	2.407	0.2962 ± 0.0053	0.4381	0.4415	For experiments with
^{252}Cf	3.756	0.1463 ± 0.0010	0.4449	± 0.0034	^{235}U sample

Probability C can be represented as follows:

$$C = \sum_{\nu=0}^{\infty} (1-\varepsilon)^{\nu} P(\nu) \qquad (9)$$

where ε is the average efficiency of the detector for recording one fission neutron and $P(\nu)$ the distribution of the number of neutrons per fission event. Table 1 gives the values of ε obtained from the experimental values of $C(C_{exp})$ and from expression (9) on the assumption that the dispersion of distribution $P(\nu)$ is 1 [10].

In Fig. 8 the function $C(\bar{\nu})$, determined by expression (9) for average experimental values of $\bar{\varepsilon}$, is shown as a straight line.

It will be seen from Table 1 and Fig. 8 that all the experimental data on C are nicely self-consistent and that expression (9) quite satisfactorily describes $C(\bar{\nu})$.

Subsequently the following values of probability C were used in deriving α:

$$C_{^{239}Pu} = 0.2955 \pm 0.0073$$
$$C_{^{235}U} = 0.2962 \pm 0.0053.$$

Expression (9) was used to make a small correction in C for the dependence of $\bar{\nu}$ on neutron energy.

The difference in C for the chamber and the sample - associated with multiplication of fission neutrons - does not exceed 10% of the measurement error in C for the samples used in these experiments and was accordingly ignored, in view of the smallness of the effect.

B. Measurement of time spectra

The time spectra of N_1 and N_2 events were measured in two ways: on a continuous spectrum (in the 10-70 keV neutron energy range) and with monochromatic neutrons.

Figs 7 and 9 show, respectively, the time spectra obtained with the ^{239}Pu sample in a three-hour series of experiments on a continuous neutron spectrum and in a half-hour experiment with 500 keV monochromatic neutrons.

The most important problem in measuring time spectra is to determine the background level. The background consists of two components: (1) a constant background due to the radioactivity of the sample and cosmic rays, constituting 20% of the total background, and (2) a background associated with neutron absorption in the collimator and neutron scattering in the sample. Owing to the high repetition rate of neutron bursts there is strong averaging of the background due to neutrons and its dependence on the time of flight is not great. The behaviour of the background level as a function of neutron time of flight was determined in these experiments with the equivalent scatterer. Fig. 7 shows the dependence (reduced to 1) of the background due to neutrons for the scatterer equivalent to the ^{239}Pu sample. The continuous curve thus obtained was used to determine the background in the working spectra. The background level was determined for each spectrum for the time interval in which neutrons had not yet reached the sample. The background in the time spectra of N_1 and N_2 events, determined by this method, is shown by a dotted curve in Figure 7.

It should be pointed out that the low effect-to-background ratio in the neutron energy range < 30 keV imposes rigorous requirements on the differential non-linearity of the apparatus. Special verification showed that the apparatus used by us did not possess systematic differential non-linearity when the statistical accuracy of the number of pulses accumulated in one channel was less than 0.3%, and the spread of points in the experimental spectra shown in Fig. 7 is statistical in nature.

On the continuous neutron spectrum we carried out nine series of measurements with the ^{239}Pu sample and five series with the ^{235}U sample, which were similar to those shown in Fig. 7. The value of probability P in these experiments, measured in each series to within ~ 1% was 0.03-0.055.

C. Measurement of amplitude spectra

The amplitude spectra of detector pulses associated with the recording of capture and fission events were measured only for the 30-70 keV neutron energy range, since it has been shown experimentally [6] that these spectra remain unchanged over a wide neutron energy range when a scintillation tank is used.

From the four amplitude spectra obtained in the experiment we can derive amplitude spectra for N_1 and N_2 events which are linked with the desired spectra by relations easily derived from expressions (1) and (2):

$$A_c = \frac{A_1 - (A_1 + A_2)\, C(1 - P)}{(1 - P) \quad (1 - C)} \tag{10}$$

$$A_f = \frac{A_2 - (A_1 + A_2)\, P}{(1 - P)\,(1 - C)} \tag{11}$$

Figure 10 shows amplitude spectra for ^{239}Pu which have been treated in this manner and averaged over several series of measurements.

The ultimate purpose of measuring the amplitude spectra is to obtain a ratio of the fractions of the spectra lying above the threshold at which the time spectra were measured. Extrapolation of the spectra to the zero threshold (needed to obtain f_f and f_c) is shown in the figure by a continuous line. The correctness of the extrapolation procedure was verified by measuring the amplitude spectrum of fission events for ^{252}Cf (Fig. 11), where the total number of fissions was measured with a fission ionization chamber. The total number of pulses in the extrapolated spectrum in Fig. 11 coincides with the number recorded by the fission chamber to within ± 1%. This is a good confirmation of the earlier evaluations of ε_{of} and demonstrates that no serious errors were made in the extrapolation procedure. The hatched area in the amplitude spectra in Fig. 10 represents the evaluated indeterminacy of the extrapolation.

The ratio of spectrum fractions for ^{239}Pu and ^{235}U obtained from amplitude spectrum analysis was

$$\frac{f_f}{f_c} = 1.01 \pm 0.05$$

Considering the earlier evaluations of ε_{oc} and ε_{of}, we used the ratio of efficiencies for recording fission and capture events in deriving α:

$$\frac{\varepsilon_{\gamma f}}{\varepsilon_{\gamma c}} = 1.08 \pm 0.07$$

D. Experimental results on the value of α

The values of N_1/N_2 and P obtained from time spectrum measurements and the measured constants of the experimental unit, C and $\varepsilon_{\gamma f}/\varepsilon_{\gamma c}$, were used for calculating α by formula (3). Each series was treated separately. Tables II and III and Figs 12 and 13 present the resulting values of α obtained by averaging the values for all series of measurements. The figures and the third column of the tables give the root-mean-square errors in the average values of α: these characterize the error in α as a function of neutron energy and do not include any indeterminacy in the constants of the experimental facility. The total root-mean-square error in the value of α, including the error in measuring C, P and $\varepsilon_{\gamma f}/\varepsilon_{\gamma c}$, is given in the fourth column of the tables. In the case of ^{235}U a correction was made for the ^{238}U impurity contained in the sample.

The figures also show most of the experimental data now available for the 10 keV-1 MeV energy range. Note the satisfactory agreement between all data obtained by similar methods using a Van de Graaff accelerator. It should, however, be pointed out that for the work reported in Refs [5], [6] and [11] much thicker samples (about six times thicker) were used, so that if a detailed comparison were attempted it would probably be necessary to take into account the possible effects of resonance self-shielding.

The rather large fluctuations in α as a function of neutron energy, in both ^{239}Pu and ^{235}U, naturally attract attention. Similar fluctuations can be found in the results of de Saussure et al. [11], although the statistical accuracy of the experimental data used by them is not sufficient to provide confirmation. Such fluctuations in the value of α are not unexpected and may be associated with irregularities in the behaviour of the fission cross-section, such as were observed recently in the fission cross-section of ^{235}U [12]. However, in the neutron energy region where our results show fluctuations in the behaviour of α, the signal-to-background ratio in the radiative capture channel is about 0.1; so these effects may be due to some unverifiable experimental factors, especially systematic errors in the background measurement. To elucidate the nature of these fluctuations, it might be useful to perform additional measurements of the relative behaviour of the fission cross-section in the same experimental conditions in which the α measurements were carried out.

In conclusion, the authors express their gratitude to A.I. Leipunsky, L.N. Usachev and A.I. Abramov for their constant interest and help in the present work.

V.S. Shorin and M.V. Bokhovko played a large part in preparing and conducting the experiments and in processing the results. The rolling and sealing of the ^{239}Pu sample was carried out by N.S. Kosulin. The operating team of the EG-1 accelerator provided a service of consistently high quality. The authors take this opportunity to express their sincere thanks to these associates for their help.

Table II

α for ^{235}U
(present work)

E_n, keV	α	$\sigma\alpha$ Relative behaviour	$\sigma\alpha$ Total error
12,4 ± 0,7	0,549	0,043	0,057
13,4 ± 0,8	0,476	0,061	0,069
14,3 ± 0,8	0,457	0,040	0,051
15,4 ± 0,9	0,531	0,032	0,048
15,9 ± 1,0	0,452	0,030	0,043
16,4 ± 1,0	0,424	0,031	0,042
16,9 ± 1,1	0,365	0,032	0,041
17,4 ± 1,1	0,350	0,026	0,036
17,9 ± 1,2	0,394	0,033	0,043
18,5 ± 1,2	0,398	0,024	0,036
19,1 ± 1,3	0,370	0,020	0,033
19,8 ± 1,4	0,338	0,029	0,038
20,4 ± 1,4	0,317	0,024	0,033
21,1 ± 1,5	0,307	0,020	0,030
21,9 ± 1,6	0,337	0,034	0,042
22,7 ± 1,7	0,339	0,021	0,031
23,5 ± 1,8	0,344	0,021	0,032
24,3 ± 1,9	0,336	0,018	0,030
25,3 ± 2,0	0,283	0,017	0,026
26,2 ± 2,0	0,268	0,019	0,027
27,3 ± 2,2	0,292	0,014	0,025
28,4 ± 2,4	0,312	0,016	0,027
29,5 ± 2,5	0,333	0,017	0,029
30,7 ± 2,7	0,346	0,019	0,031
32,1 ± 2,8	0,350	0,019	0,031
33,4 ± 3,0	0,342	0,018	0,030
34,9 ± 3,2	0,350	0,017	0,030
36,5 ± 3,4	0,340	0,020	0,031
38,2 ± 3,7	0,346	0,019	0,031
40 ± 3,9	0,332	0,019	0,030
42 ± 4,2	0,335	0,019	0,030
44,1 ± 4,6	0,308	0,011	0,025
46,3 ± 4,9	0,307	0,016	0,027
48,8 ± 5,3	0,300	0,017	0,027
51,4 ± 5,7	0,285	0,016	0,026
54,3 ± 6,2	0,288	0,018	0,027
57,4 ± 6,8	0,277	0,015	0,025

Table II (continued)

E_n, keV	α	$\sigma\alpha$ Relative behaviour	$\sigma\alpha$ Total error
60,8 ± 7,4	0,292	0,013	0,025
90 ±15	0,307	0,025	0,030
135 ±25	0,247	0,015	0,024
185 ±15	0,218	0,010	0,019
300 ±10	0,181	0,011	0,018
400 ±10	0,183	0,010	0,018
500 ±10	0,150	0,006	0,014
750 ±30	0,127	0,011	0,012
900 ±30	0,101	0,010	0,014
1100 ±30	0,077	0,009	0,013

Table III

α for ^{239}Pu
(present work)

E_n, keV	α	$\sigma\alpha$ Relative behaviour	$\sigma\alpha$ Total error
9,4 ± 0,5	0,502	0,079	0,035
10,4 ± 0,5	0,508	0,058	0,067
11,3 ± 0,6	0,572	0,041	0,055
12,2 ± 0,7	0,517	0,068	0,076
13,1 ± 0,7	0,538	0,077	0,034
14,2 ± 0,8	0,478	0,037	0,048
15,2 ± 0,9	0,418	0,054	0,061
15,9 ± 1,0	0,366	0,038	0,045
16,4 ± 1,0	0,342	0,042	0,049
16,8 ± 1,1	0,331	0,032	0,040
17,3 ± 1,1	0,325	0,028	0,037
17,9 ± 1,2	0,329	0,030	0,038
18,4 ± 1,2	0,316	0,026	0,035
19,0 ± 1,3	0,328	0,031	0,039
19,6 ± 1,4	0,340	0,025	0,034
20,3 ± 1,4	0,352	0,032	0,040
20,9 ± 1,5	0,346	0,021	0,032
21,6 ± 1,6	0,369	0,018	0,030
22,4 ± 1,7	0,348	0,015	0,029
23,2 ± 1,7 0,	0,346	0,022	0,033

Table III (continued)

E_n, keV	α	σα Relative behaviour	σα Total error
24,0 ± I,8	0,320	0,0I8	0,029
24,8 ± I,9	0,3I6	0,0I5	0,027
25,8 ± 2,0	0,330	0,022	0,032
26,7 ± 2,2	0,302	0,0I7	0,027
27.8 ± 2,3	0,293	0,0I5	0,026
28,8 ± 2,4	0,282	0,02I	0,030
30,0 ± 2,6	0,247	0,0II	0,022
3I,2 ± 2,7	0,258	0,0II	0,022
32,5 ± 2,9	0,272	0,0I2	0,024
33,9 ± 3,I	0,286	0,0I6	0,026
35,3 ± 3,3	0,260	0,0I5	0,025
36,9 ± 3,5	0,260	0,009	0,022
38,6 ± 3,4	0,243	0,0II	0,022
40,4 ± 4,0	0,247	0,0I4	0,024
42,3 ± 4,3	0,240	0,0I0	0,02I
44,3 ± 4,6	0,225	0,007	0,020
46,5 ± 4,9	0,2I3	0,006	0,0I9
48,9 ± 5,3	0,207	0,009	0,020
5I,4 ± 5,7	0,I93	0,007	0,0I8
54,2 ± 6,2	0,I76	0,008	0,0I8
57,2 ± 6,7	0,I74	0,007	0,0I8
60,4 ± 7,3	0,I70	0,005	0,0I7
64 ± 8,0	0,I72	0,006	0,0I7
II0 ±20	0,I49	0,C07	0,0I5
I50 ±25	0,II5	0,0I0	0,0I6
I85 ±I5	0,090	0,009	0,0I5
300 ±I0	0,I03	0,0I2	0,0I8
400 ±I0	0,075	0,009	0,0I5
500 ±I0	0,082	0,0I0	0,0I5
750 ±30	0,07I	0,009	0,0I5
900 ±30	0,032	0,006	0,0I2
I000 ±30	0,008	0,0I3	0,0I7

REFERENCES

[1] GREEBLER, P., et al., Nucl. Application No. 5 (1968) 297.

[2] SPIVAK, P.E., EROZOLIMSKY, B.G., DOROFEEV, G.A., LAVRENCHIK, V.N., KUTIKOV, I.E., DOBRYNIN, Yu.P., Atomn. Energ. 3 (1956) 21.

[3] ANDREEV, V.N., Atomn. Energ. 4 (1958) 185.

[4] VANKOV, A.A., STAVISSKY, Yu.Ya., Atomn. Energ. 19 (1965) 41.

[5] HOPKINS, J.C., DIVEN, B.C., Nucl. Sc. Eng. 12 (1962) 169.

[6] WESTON, L.W., de SAUSSURE, G., GWIN, R., Nucl. Sc. Eng. 20 (1964) 80.

[7] VOLODIN, V.I., GLOTOV, A.I., DUDKIN, N.I., KANAKI, V.N., KONONOV, V.N., METLEV, A.A., ROMANOV, V.A., Paper presented at the Second All-Union Conference on charged-particle accelerators [in Russian], Moscow (1970).

[8] KONONOV, V.N., METLEV, A.A., POLETAEV, E.D., PROKOPETS, Yu.S., Priborÿ tekh. éksp. 6 (1969) 51.

[9] SIEGBAHN, K. (Ed.), Alfa-, beta- and gamma-spectroscopy [in Russian], Atomizdat (1969).

[10] MARION, D., FOWLER, D. (Eds), Fast Neutron Physics [Russ. ed. Atomizdat Vol. 2 (1966) 704].

[11] de SAUSSURE, G., et al. Nucl. Data for Reactors V.II, p. 233, IAEA, Vienna (1967).

[12] PATRICK, B.H. et al. AERE - R 6350 (1970).

[13] GWIN, R. et al. Nucl. Sc. Eng. 40 (1970) 306.

[14] SCHOMBERG, M.G. et al. in Nuclear Data for Reactors (Proc. Conf. Helsinki 1970), I, IAEA, Vienna (1970) 315.

[15] CZIRR, J.B. et al., ibid., p. 331.

[16] RYABOV, Yu.V., SO DON SIK, CHIKOV, N., KUROV, M.A., Preprint R3-5113, Dubna (1970).

[17] VAN-SHI-DI, VAN YUN-CHAN, DERMENDZHIEV, E., Physics and Chemistry of Fission (Proc. Symp. Salzburg 1965) I, IAEA, Vienna (1965) 287.

[18] KONONOV, V.N., KUROV, M.A., POLETAEV, E.D., PROKOPETS., Yu.S., RYABOV, Yu.V., SO DON SIK, STAVISSKY, Yu.Ya., CHIKOV, N., Preprint R3-5112, Dubna (1970).

FIGURE CAPTIONS

Fig. 1. Diagram of the experimental facility.

Fig. 2. Distribution of fission neutron lifetimes in the detector.

Fig. 3. Efficiency of recording single gamma-quanta at zero threshold as a function of gamma-quantum energy.

Fig. 4. Efficiency of recording a cascade of gamma-quanta as a function of multiplicity for a total cascade energy of 6.4 MeV at zero recording-threshold.

Fig. 5. Block diagram of the circuit used in measuring time spectra.

Fig. 6. Block diagram of the circuit used in measuring amplitude spectra.

Fig. 7. The time spectra of the apparatus: a - time spectrum of N_1 events (mainly radiative capture) for the ^{239}Pu sample; b - time spectrum of N_2 events (mainly fission) for the ^{239}Pu sample; c - reduced background due to the neutron beam for a scatterer equivalent to the plutonium sample (N_1).

Fig. 8. Probability C as a function of the average number of neutrons per fission event: a - in experiments with the ^{239}Pu sample (threshold for recording fission neutrons ~0.9 MeV); b - in experiments with the ^{235}U sample (threshold for recording fission neutrons ~0.5 MeV).

Fig. 9. Apparatus time spectra of N_1 (a) and N_2 (b) events in the experiment with 500 keV mono-energetic neutrons.

Fig. 10. [missing]

Fig. 11. Amplitude spectrum of detector pulses in recording spontaneous fissions of ^{252}Cf from prompt fission gamma-rays.

Fig. 12. Value of α for ^{235}U as a function of neutron energy.

Fig. 13. Value of α for ^{239}Pu as a function of neutron energy.

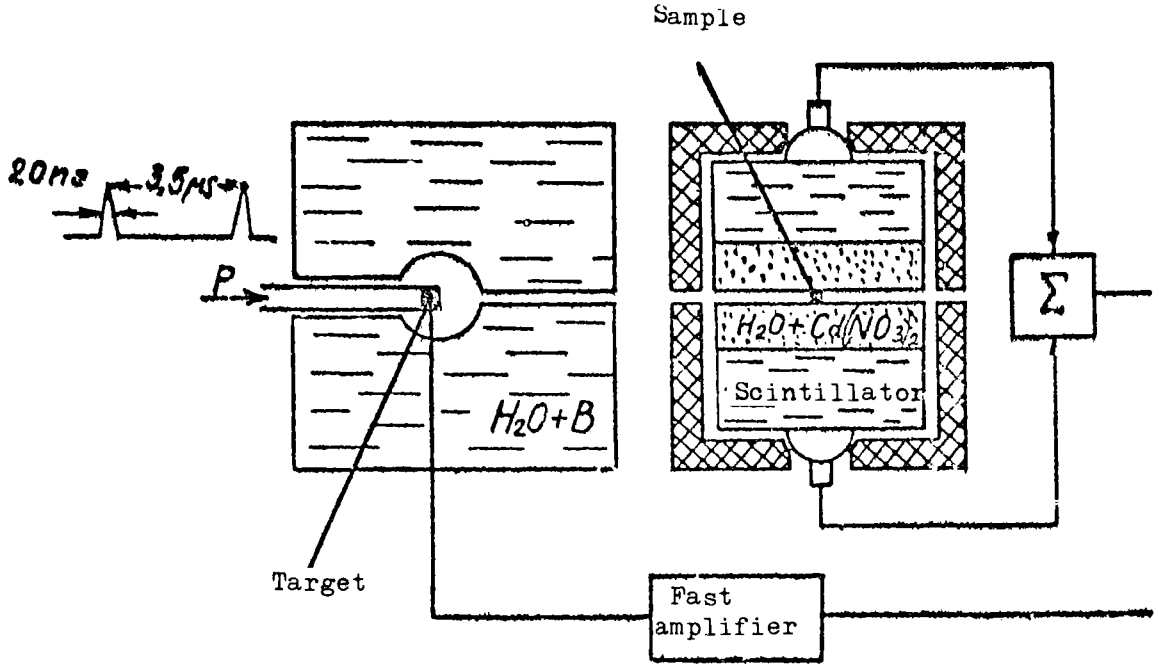
Sample
20ns
3,5μs
P
H_2O+B
$H_2O+Cd(NO_3)_2$
Scintillator
Σ
Target
Fast
amplifier

Figure 1

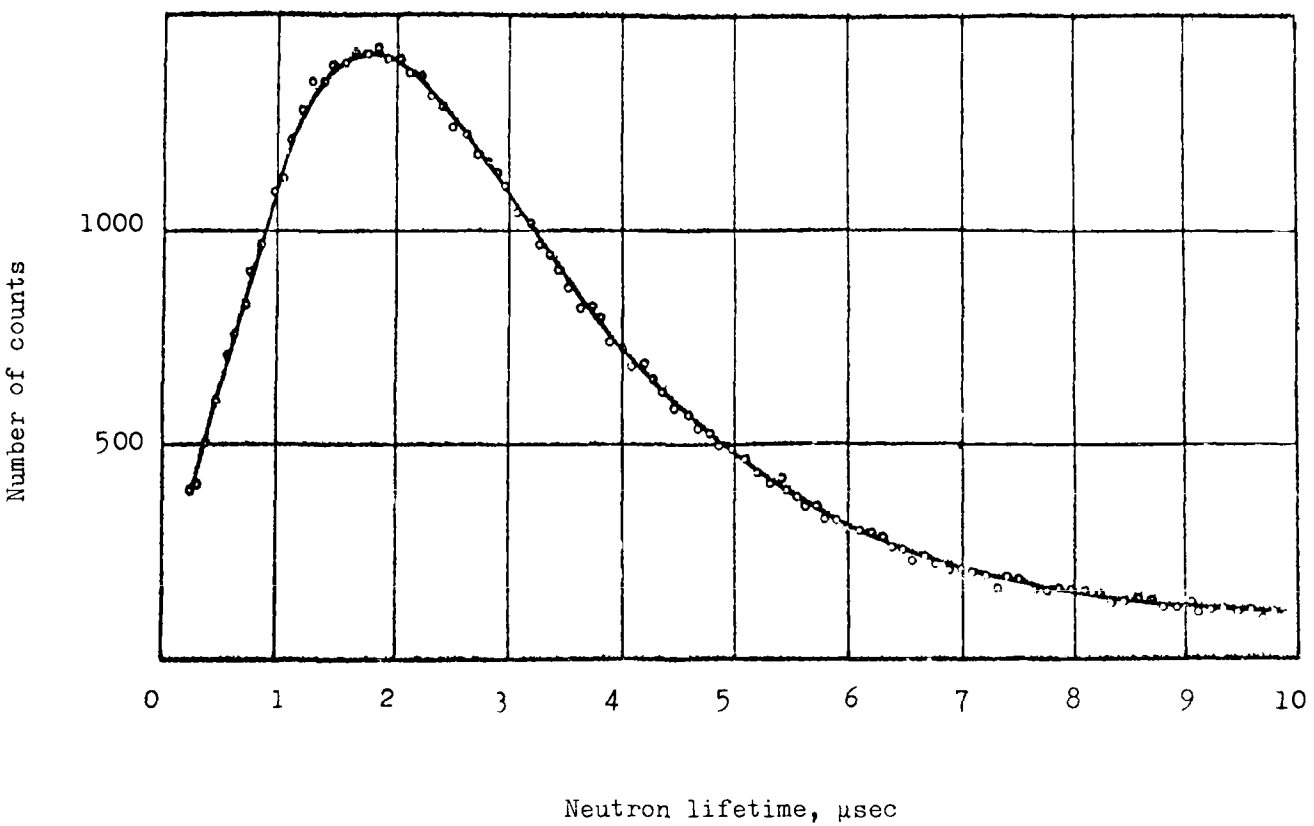
Number of counts
1000
500
0
1
2
3
4
5
6
7
8
9
10
Neutron lifetime, μsec

Fig. 2

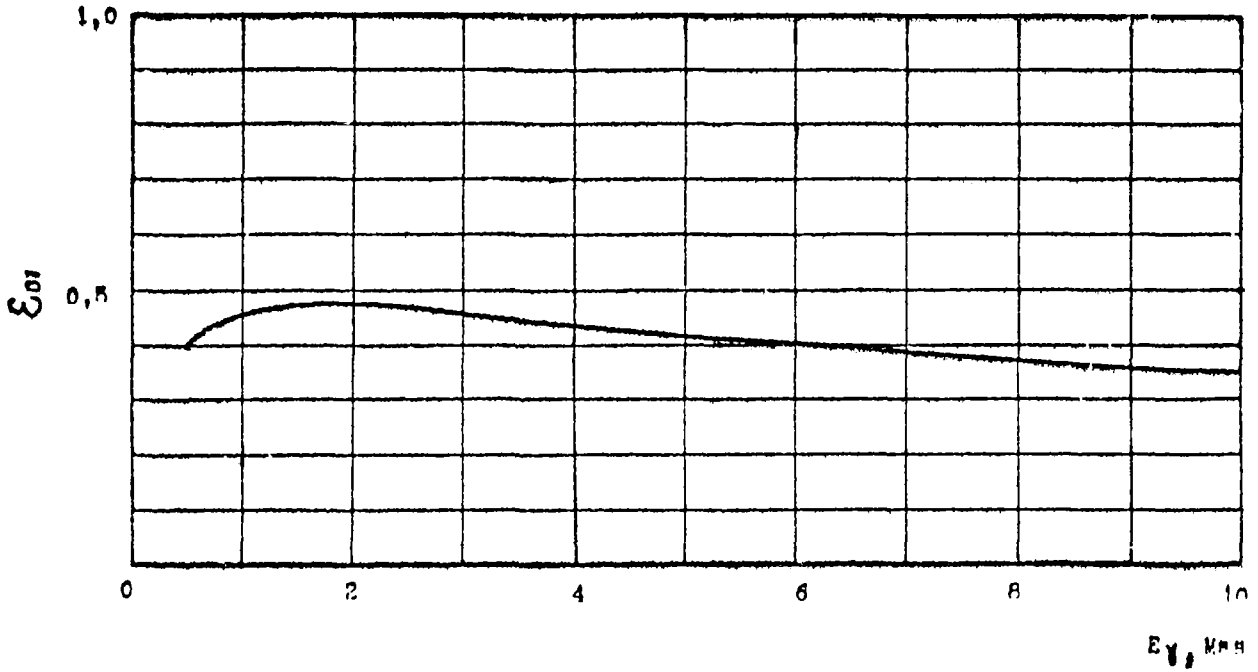

Fig. 3

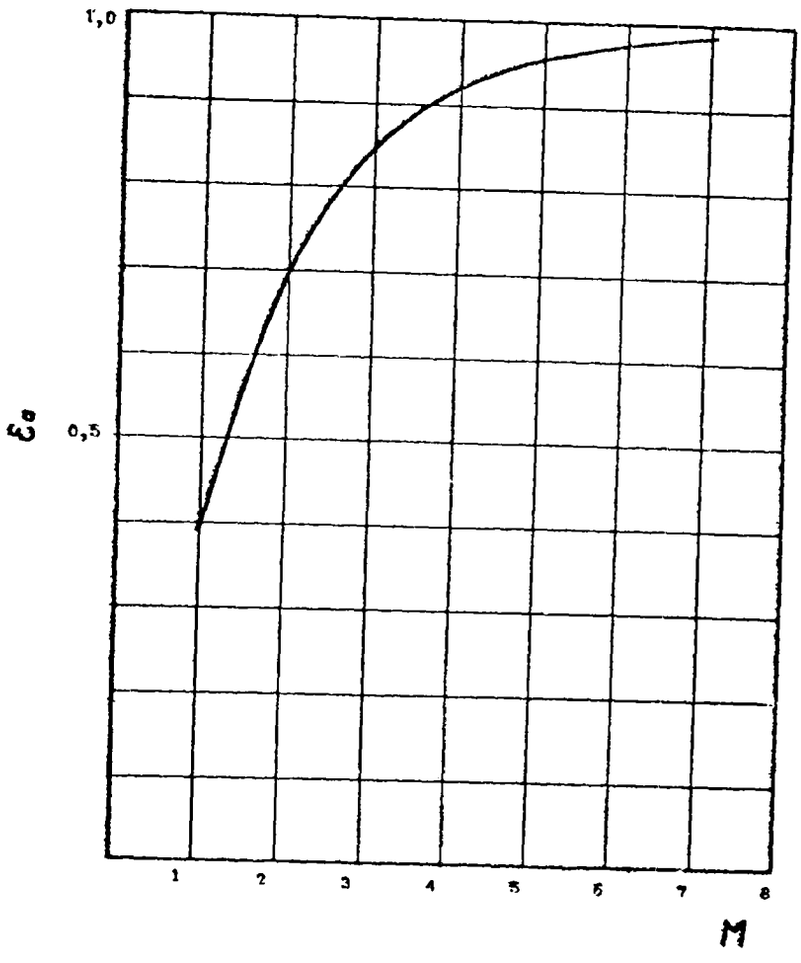

Fig. 4

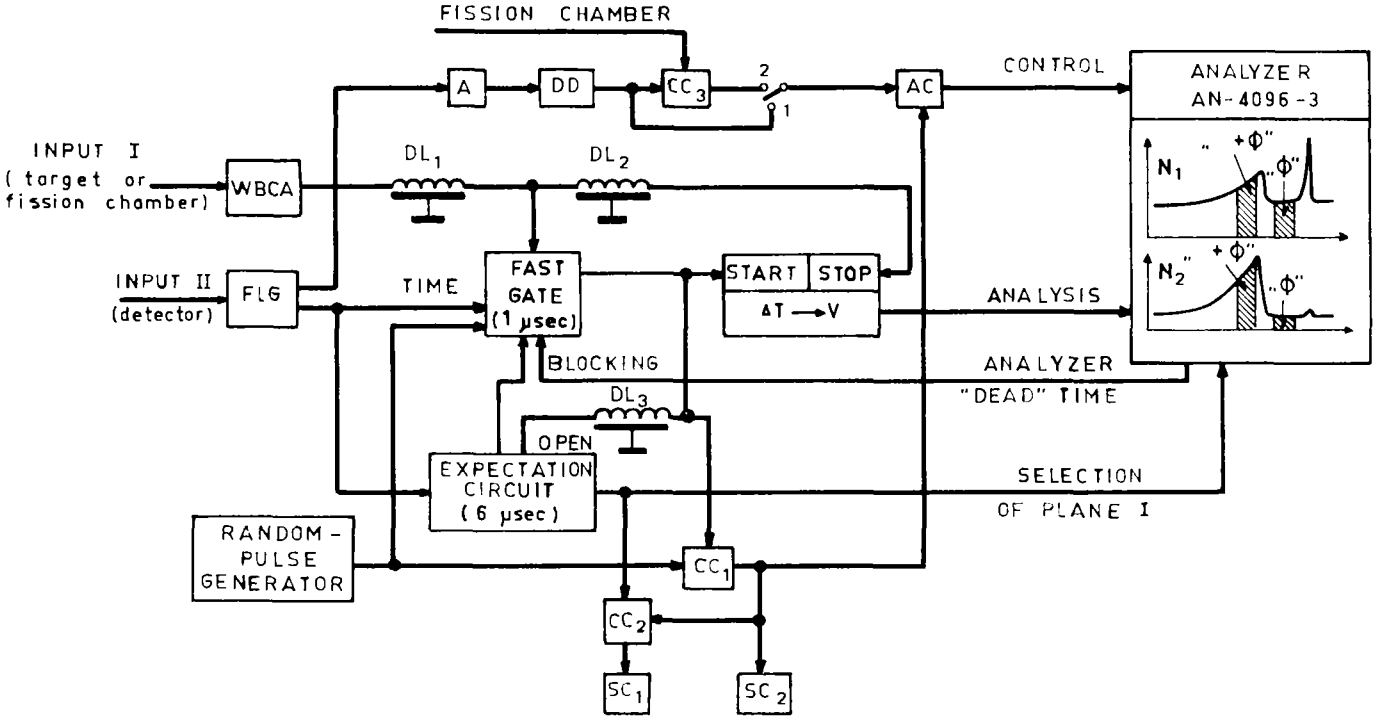
FISSION CHAMBER
A
DD
CC3
2
1
AC
CONTROL
ANALYZER
AN-4096-3
INPUT I
(target or
fission chamber)
WBCA
DL1
DL2
INPUT II
(detector)
FLG
TIME
FAST
GATE
(1 μsec)
START
STOP
ΔT → V
ANALYSIS
BLOCKING
ANALYZER
"DEAD" TIME
DL3
OPEN
EXPECTATION
CIRCUIT
(6 μsec)
SELECTION
OF PLANE I
RANDOM-
PULSE
GENERATOR
CC1
CC2
SC1
SC2
N1
+Φ"
Φ"
N2"

Fig. 5

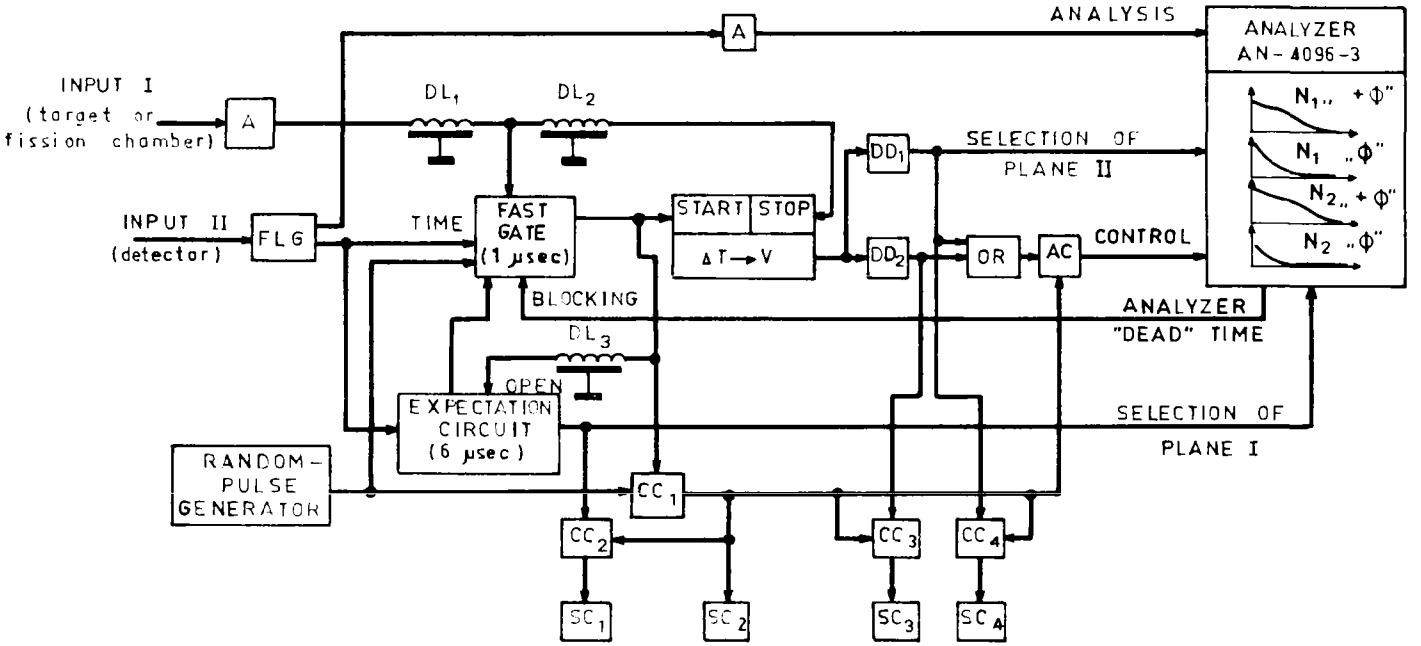
ANALYSIS
ANALYZER
AN-4096-3
A
INPUT I
(target or
fission chamber)
A
DL1
DL2
DD1
SELECTION OF
PLANE II
INPUT II
(detector)
FLG
TIME
FAST
GATE
(1 μsec)
START
STOP
ΔT→V
DD2
OR
AC
CONTROL
BLOCKING
ANALYZER
"DEAD" TIME
DL3
OPEN
EXPECTATION
CIRCUIT
(6 μsec)
SELECTION OF
PLANE I
RANDOM-
PULSE
GENERATOR
CC1
CC2
CC3
CC4
SC1
SC2
SC3
SC4

Fig. 6

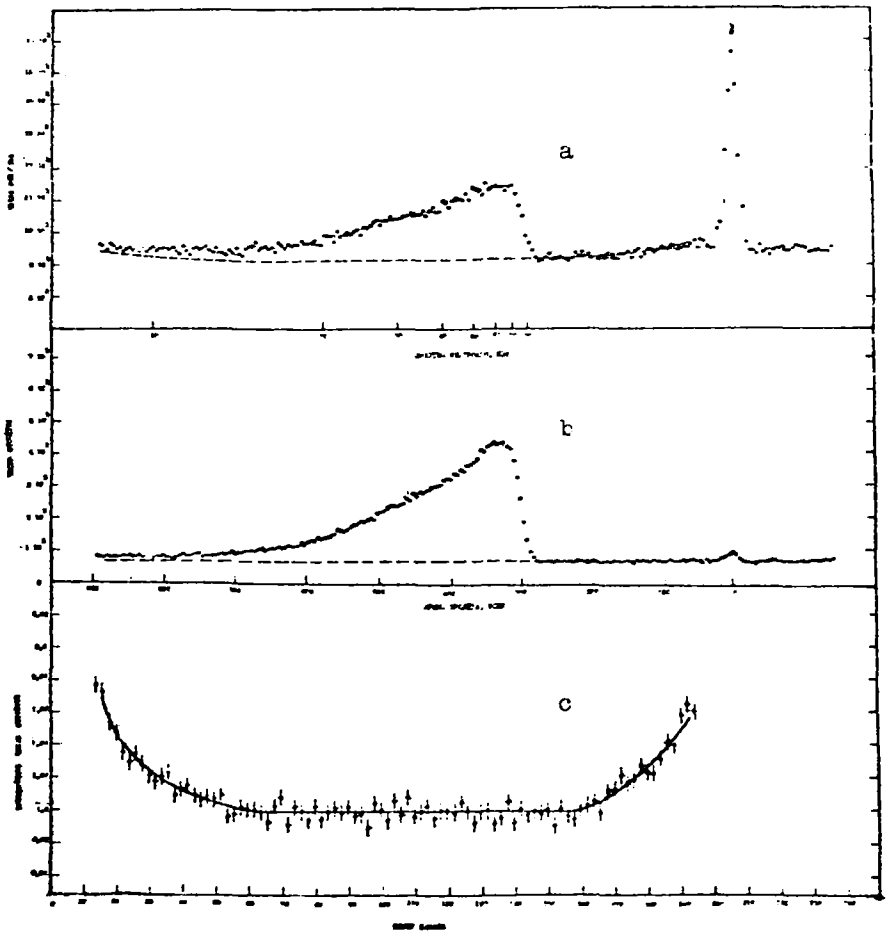

Fig. 7

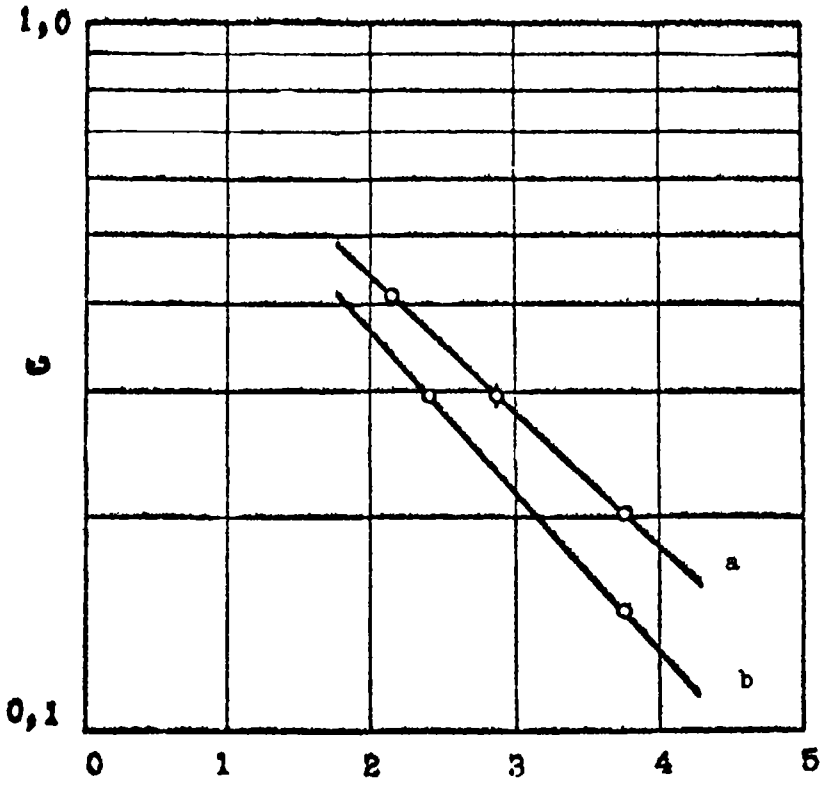

Average number of prompt neutrons ν

Fig. 8

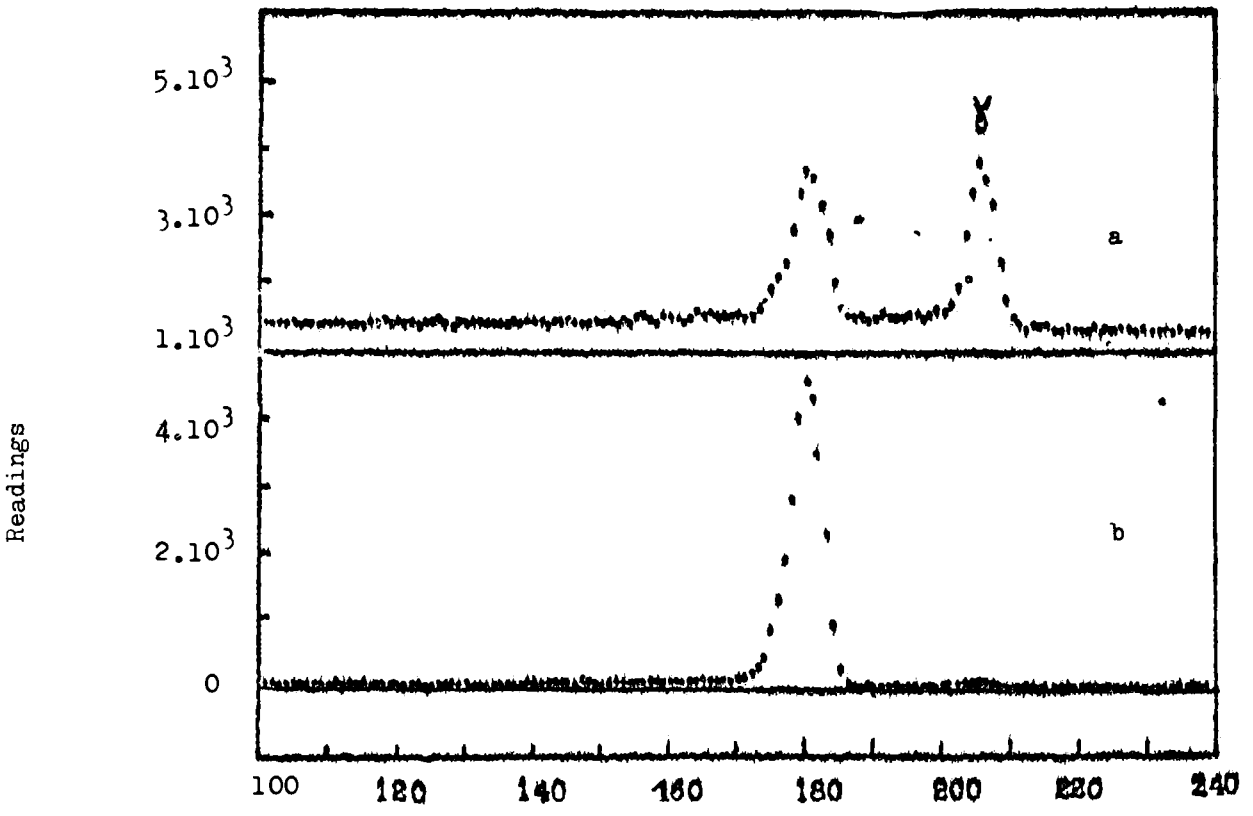
5.10³
3.10³
1.10³
4.10³
2.10³
0
a
b
100
120
140
160
180
200
220
240
Readings
Channel number

[Fig. 10 missing]

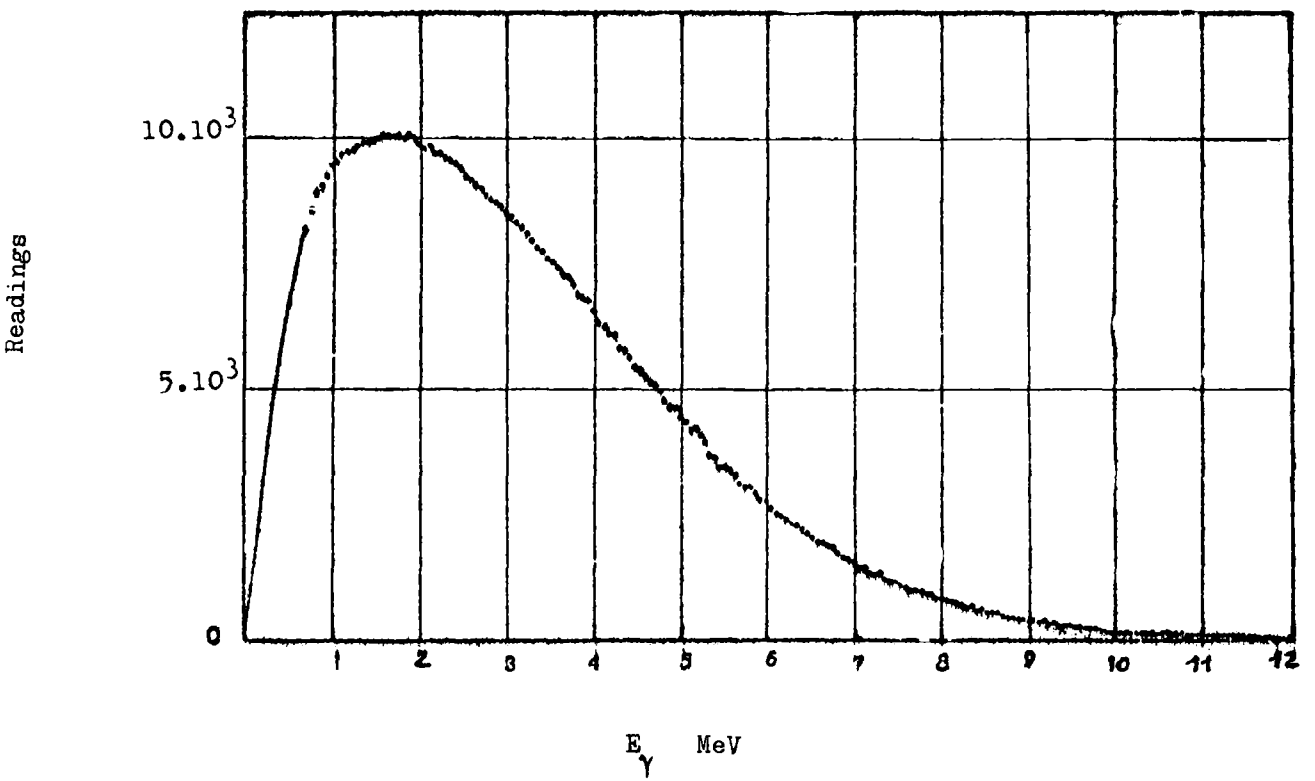

Fig. 11

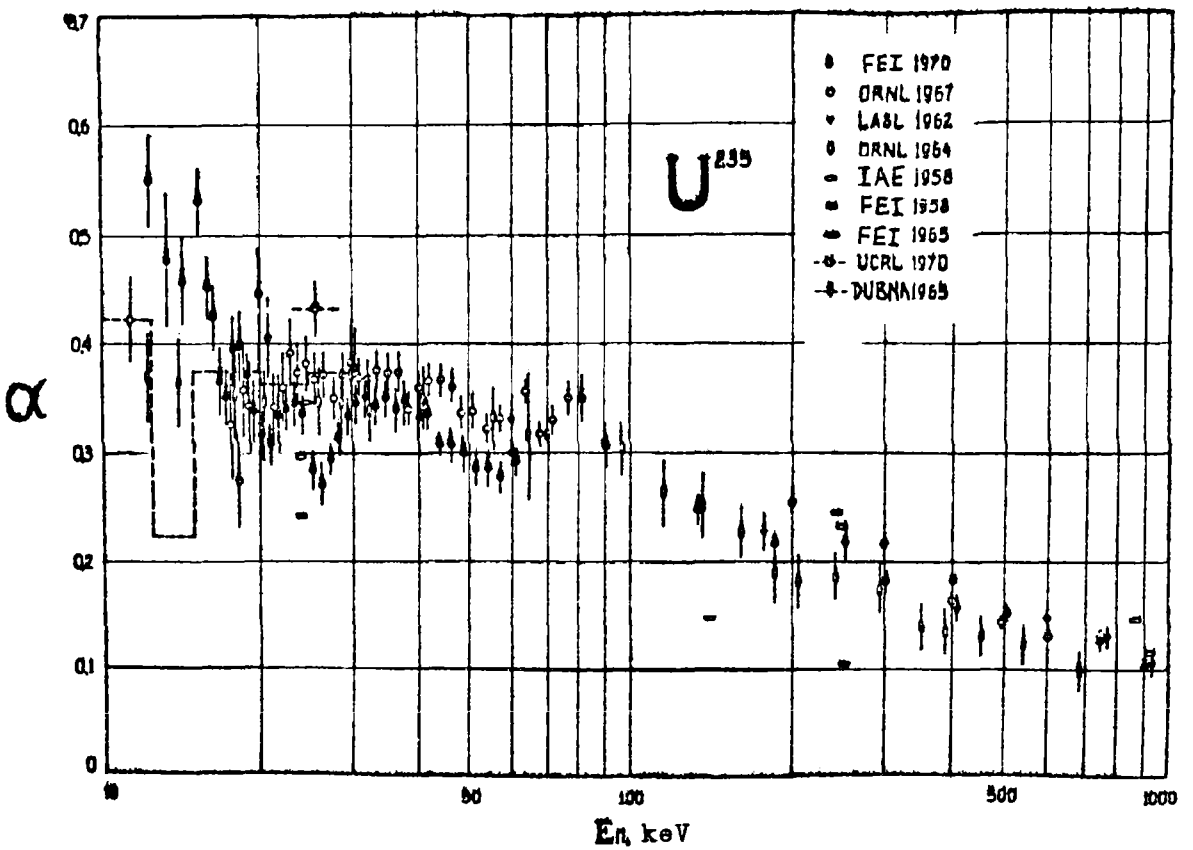

Fig. 12 • - present work

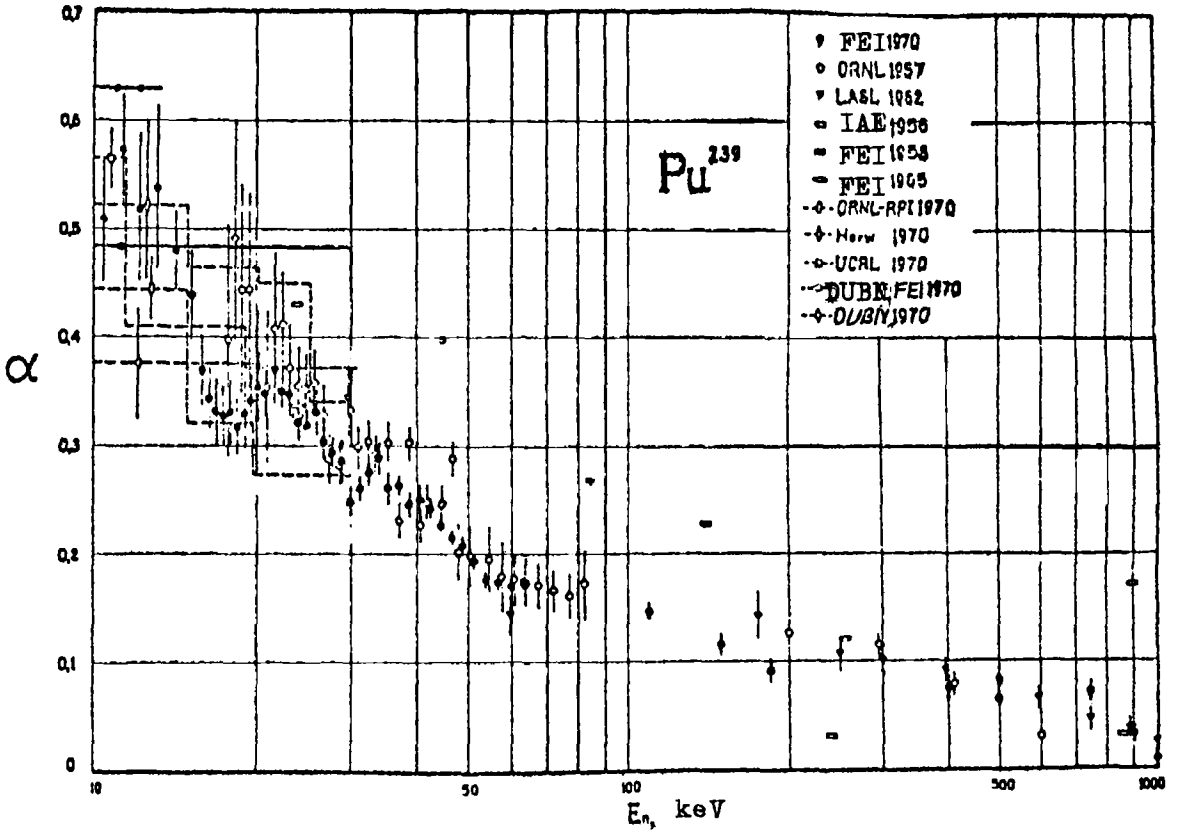

Fig. 13 • - present work